Membrane and Water Treatment, *Vol. 13, No. 1 (2022) 29-37*
https://doi.org/10.12989/mwt.2022.13.1.029

Engineered nanoparticles in wastewater systems: Effect of organic size on the fate of nanoparticles

Soohoon Choi**[1,2], Ching-Lung Chen[1,3,4], Murray V. Johnston[5], Gen Suh Wang[6] and Chin-Pao Huang*[1]

[1]*Department of Civil and Environmental engineering, University of Delaware, Newark, DE 19711, USA*
[2]*Department of Environmental Engineering, Chungnam University, 99 Daehak-ro, Yuseong-gu, Daejeon 34134, Korea*
[3]*Department of Safety, Health and Environmental Engineering, Ming Chi University of Technology, New Taipei City, 24301, Taiwan*
[4]*Center for Environmental Sustainability and Human Health, Ming Chi University of Technology, New Taipei City, 24301, Taiwan*
[5]*Department of Chemistry and Biochemistry, University of Delaware, Newark, DE 19711, United States*
[6]*Institute of Environmental Health, National Taiwan University, Taipei 100, Taiwan*

(Received May 31, 2021, Revised August 10, 2021, Accepted September 3, 2021)

Abstract. To verify the fate and transport of engineered nanoparticles (ENP), it is essential to understand its interactions with organic matter. Previous research has shown that dissolved organic matter (DOM) can increase particle stability through steric repulsion. However, the majority of the research has been focused on model organic matter such as humic or fulvic acids, lacking the understanding of organic matter found in field conditions. In the current study, organic matter was sampled from wastewater treatment plants to verify the stability of engineered nanoparticles (ENP) under field conditions. To understand how different types of organic matter may affect the fate of ENP, wastewater was sampled and separated based on their size; as small organic particular matter (SOPM) and large organic particular matter (LOPM), and dissolved organic matter (DOM). Each size fraction of organic matter was tested to verify their effects on nano-zinc oxide (nZnO) and nano-titanium oxide ($nTiO_2$) stability. For DOM, critical coagulation concentration (CCC) experiments were conducted, while sorption experiments were conducted for organic particulates. Results showed that under field conditions, the surface charge of the particles did not influence the stability. On the contrary, surface charge of the particles influenced the amount of sorption onto particulate forms of organic matter. Results of the current research show how the size of organic matter influences the fate and transport of different ENPs under field conditions.

Keywords: attachment; critical coagulation concentration; dissolved organic matter; fate and transport; TiO_2 and ZnO nanoparticles

1. Introduction

During the last decade, engineered nanoparticles (ENP) have become an essential part of everyday consumer products, exhibiting a widespread application in foods, personal care products, textiles, and home appliances (Benn and Westerhoff 2008, Nowack *et al*. 2011, Weir *et al*. 2012, Windler *et al*. 2012, Hansen *et al*. 2016, Wagener *et al*. 2016). Studies have shown various pathways of exposure of these particles into the aquifer, ranging from municipal waste to non-point source pathways (Kaegi *et al*. 2008, Benn *et al*. 2010, Petersen *et al*. 2011, Debia *et al*. 2016). And based on the product type and property, some show as much as 100% direct release into the sewer system, where some show a small but steady release of particles under specific conditions. The outflow of ENPs will undergo various treatment procedures, eventually resulting in exposure to aquatic life forms as well as landfill accumulation (Adams *et al*. 2006, Bolyard *et al*. 2013, Sun *et al*. 2016, Bundschuh *et al*. 2018).

In aquatic environments, the transport and fate of nanoparticles are mainly due to the mobility of the particles. Interaction between particles play a key role in determining the behavior, mobility, and fate of ENP. According to the DLVO theory, the rate of aggregation kinetics depends on the electrostatic double layer of the particles. With the increase of ionic strength, electric double layer compression occurs, lowering the resistance between the particles, resulting in a higher likelihood of particle attachment. The stability ratio (or attachment efficiency) shows the particle attachment as a function of ionic strength concentrations. Aside from DLVO forces, organic sorption onto nanoparticle surfaces increases the stability of particles through steric repulsion. Negatively charged functional groups on the organic matter causes steric repulsion, resulting in the stability of the nanoparticles, decreasing the aggregation kinetics and hence increases the CCC values (Li and Chen 2012, Miao *et al*. 2016). As an example, it has been reported that with the addition of humic acids, the CCC values of SWCN was increased 2~5 times (Chen and Elimelech 2007). The influence of organic matter relies on the type of organic matter as well as the amount sorbed onto the particle surface. It has been known that the type of organic matter influences the stabilization of particles, where humic acid (HA) showed the highest repulsion

*Corresponding author, Professor,
E-mail: huang@udel.edu
**Co-corresponding author, Professor,
E-mail: crimson@cnu.ac.kr

ISSN: 2005-8624 (Print), 2092-7037 (Online)

followed by natural organic matter (NOM) and fulvic acids (FA) (Erhayem and Sohn 2014). The amount of organic sorption to the particle surface also follows this order, where the sorption of organic matter is due to the higher ratio of aromatic to aliphatic carbon (Erhayem and Sohn 2014). In general, an increase in organic sorption will enhance the stability of particles; however, it has been proven that at low organic concentrations aggregation processes were increased through organic bridging (Illés and Tombácz 2006). This has been observed with the existence of divalent cations, where Ca^{2+} induced a bridging effect between the sorbed organic materials resulting in faster aggregation kinetics (Li and Huang 2010).

Various aggregation studies have been conducted with different ENPs (ZnO, TiO_2, Fe_2O_3, C60, Single walled carbon nanotubes and grapheme oxide) under numerous aquatic conditions to verify the fate and transport of nanoparticles (Chen and Elimelech 2006, Zheng *et al*. 2011, Aboubaraka *et al*. 2017, Chang *et al.* 2017, Sani-Kast *et al*. 2017, Sousa *et al*. 2017). Both metallic and carbon based nanoparticles show similar characteristics under higher ionic strengths as well as sorption of dissolved organic material onto the particle surface. With NaCl, the CCC values of carbon based nanoparticles range from 44~160 mM, where metallic particles ranging from 20~40 mM (Keller *et al*. 2010, Li and Huang 2010, Chowdhury *et al*. 2013, Jiang *et al.* 2016). Difference in the measured CCC range are due mainly to the surface characteristics of the particles, where metallic oxides have an even charge distribution on the surface where the carbon based nanoparticles differ on the state of surface oxidation. Detailed results of the literature research showed CCC values of 25, 15, 20, 160, 160, and 44 mM for TiO_2, Fe_2O_3, C_{60}, SWCN, and GO respectively (Illés and Tombácz 2006, Chen and Elimelech 2007, Chen *et al*. 2007, Li and Huang 2010, Zhou and Keller 2010, Jiang *et al.* 2016).

For carbon-based materials it has been proven that the surface charge relies on the oxidation of the carbon surfaces leading to surface functional groups (Duch *et al*. 2011). Carboxylic and hydroxyl functional groups are the main cause of the surface charge of carbon materials, where the amount of oxidation determines the degree of surface charge and hence the aggregation (Jiang *et al*. 2016). However, some studies have shown that the shape of materials also influences the aggregation of the particles. This has been seen in carbon nanotubes having structural irregularities in its scaffold as well as incomplete carbon rings in the end termini, making it more acceptable to oxidation (Müller and Bunz 2007). Graphene oxide and fullerenes also share this trend where the CCC value of 2D graphene oxide (GO) is higher than 1D carbon nanotubes (CNT), and lower than 3D fullerene (Chowdhury *et al*. 2013). Among graphene oxides, the physical crumbling of the particles also showed influence on the surface charge and attachment characteristics (Jiang *et al*. 2016). Difference in CCC values based on particle shape has also been seen with ZnO, where non-spherical particles show faster aggregation characteristics compared to spherical particles (van Zanten and Elimelech 1992).

Various studies have proven the effect of humic, fulvic and NOM on the stability of ENP. However, the majority of the research was focus was on controlled organic substances with the lack of investigation in field samples. In the current study, particle stability was investigated under aquatic conditions that simulate wastewater treatment plants. Organic matter used in the study was extracted from field samples collected from wastewater treatment plants to verify the particle stability under dissolved organic matter and attachment to sludge particulates. The pH and ionic strength will be a main factor as well as the natural organic matter from the sampled wastewater. Attachment efficiency tests were conducted to verify the effects of natural wastewater conditions and its effect on the stability and aggregation of the nanoparticles of interest. Additionally, sorption tests of two different size fractions with ENP were also conducted to assess the amount of organic sorption to nanoparticles, and its fate as well.

2. Theoretical aspects

Aggregation of mono-disperse particles to doublet formation can be described with a kinetic approach with the equation (van Zanten and Elimelech 1992, Shih *et al*. 2012)

$$\frac{dN_2}{dt} = \frac{1}{2}k_{11}N_1^2 - k_{12}N_1N_2 \quad (1)$$

this equation shows the aggregation kinetics of single particle aggregation as well as the dissociation of aggregated particles, where N_1 and N_2 are the number particles of the primary and secondary particles, respectively. The second-order rate constants k_{11} and k_{12} are rate constants related to the aggregation and dissociation process of particle interaction, respectively. For early state aggregation where single particle interaction occurs, in absence of dissociation, Eq. (1) can be simplified as the following expression

$$\frac{dN_2}{dt} = -\frac{1}{2}\frac{dN_1}{dt} = \frac{1}{2}k_{11}N_1^2 \quad (2)$$

Based on the surface chemistry of the particles and aquatic chemistry, particles aggregation may display two different stages. The fast aggregation stage occurs under high salinity conditions or at pH near the ZPC of the particles where the surface charge of the particles is negligible. According to Smoluchowski, (van Zanten and Elimelech 1992) in this state, Brownian motion dominates the particle attachment where each collision results in aggregation represented by the following equation.

$$k_{11,fast} = \frac{4k_BT}{3\mu} \quad (3)$$

where k_{11fast} is the rate constant for fast aggregation, k_B is the Boltzmen constant, T is temperature, and μ is the viscosity of the fluid.

On the contrary, slow aggregation occurs under conditions where the repulsive forces retard the aggregation between the particles lowering the attachment per collision ratio. The relationship between the two stages can be explained by the following equation

$$k_{11}N_1^2 = \alpha k_{11,fast}N_1^2 \quad (4)$$

where k_{11} is the aggregation rate constant at a given aquatic condition, k11fast is the rate constant at the fast aggregation stage, and α is the attachment efficiency. The attachment efficiency is the also known as the reciprocal of the stability ratio (W), where it represents the success of attachment per number of particle collision. The equation can also be stated as

$$\alpha = \frac{1}{W} = \frac{k_{11}}{k_{11,fast}} \quad (5)$$

Through the comparison of aggregation rates, the attachment efficiency ($0 < \alpha \leq 1$) can be known without measuring the absolute rate values.

3. Material and methods

3.1 Preparation of engineered nanoparticles

For the experiments, titanium dioxide (P25, Sigma Aldrich), and zinc oxide (Sigma Aldrich, U.S.A.) was used as model ENP. According to the information provided by the supplier, TiO_2 has a diameter of 21 nm with an assay of ≥ 99.5% trace metals basis, where ZnO has a diameter of 50 nm and smaller with an assay of ≥ 97% trace metals basis. However, using dynamic light scattering (DLS), (Zetasizer nano, Malvern, UK) the hydrodynamic radius of TiO_2 particles were determined to be 200 nm (± 20 nm) and ZnO to be 80 nm (± 10 nm) in diameter when measured in aqueous conditions. Before each experiment, the powdered form of ENP was suspended in deionized water (18 mΩ) and dispersed with a high intensity ultrasound processor (Ultrasonic Homogenizer 4710 Series, Cole-Parmer Instrument Co., Chicago, IL). During the sonication process the temperature of the samples were controlled with a thermostat pump in conjunction with a cooler and adjusted to 25°C. The electrolyte (NaCl and Na_2SO_4) stock solutions were prepared and filtered through 0.2 μm filters and adjusted to the desired pH before use. All samples were, unless otherwise stated, prepared at a pH of 6.0. All chemicals were of analytical grade.

3.2 Collection and preparation of dissolved organic matter

Wastewater samples were collected from the secondary return sludge of the Wilmington wastewater treatment plant. Sampled wastewater was firmly sealed and stored in an icebox containing ice during the transportation process. The collected samples were stored in a refrigerated environment of 4°C before experiments. Experiments were conducted within three days after sampling. Organic matter was separated into three fractions based on their size; as dissolved organic matter (DOM), small organic particular matter (SOPM), and large organic particulate matter (LOPM). Centrifugation was used to separate the DOM fraction of organic matter from the sludge. Collected wastewater was centrifuged at 20,000G for 30 min (RC-5 Super-speed Refrigerated centrifuge, DuPont), to separate particular organic and other undissolved matter from the samples. The DOM was collected from the supernatant of the centrifuged wastewater samples. After collection the DOM samples were analyzed for the organic content with a TOC analyzer. Collected DOM samples were stored in a refrigerated environment before the experiments. The SOPM was collected through gravitational sedimentation, where sampled sludge was settled in an Imhoff cone for 4 hr. After the sedimentation process, the supernatant was collected for SOPM. To collect the LOPM, sludge was settled in an Imhoff cone for 4 hrs, where the settled matter was collected as the LOPM. The supernatant was removed and the settled matter was then collected to acquire the LOPM. To isolate only the organic matter that is larger than 1 μm, the settled matter in the Imhoff cone was suspended in DI water and settled to separate additional DOM and SOPM in the separated sample. The supernatant of the settled sludge was removed, and the settled matter was filled with DI water, agitated and settled for 4hours again. After the sedimentation process, the supernatant containing DOM and SOPM was removed and the Imhoff cone was again filled with DI water. This process was repeated for three times to remove as much DOM and SOPM in the sludge samples.

3.3 Coagulation experiments

The change in particle diameter was measured with Dynamic light scattering, performed on the Zetasizer nano (Malvern). It was equipped with a He-Ne laser source with a wavelength of 633 nm and 90° fixed angle detector. Before each experiment the ENP was dispersed with a high powered sonicater (Ultrasonic Homogenizer 4710 Series, Cole-Parmer Instrument Co., Chicago, IL) for a minimum of 2 minutes for maximum particle dispersion. The stock suspension of TiO_2 and ZnO were added to a disposable methacrylate cuvette (Fisherbrand, Fisher), and diluted with DI water to match the target particle concentration. The desired ionic solution was added moments before the sample was added into the cuvettes and placed in the instrument (Zetasizer) for measurement. For experiments associated to ENP and organic matter, DOM was added to the cuvettes immediately after the ENP.

The measurement was conducted with a 10 second interval with a total measurement time of 30 minutes to an hour. Total detection time was based on the time for the hydrodynamic radius to increase approximately 30%. This provides adequate data to derive the aggregation kinetics of single particle interaction, since the defective doublet hydrodynamic radius has been reported to be about 1.38 times the primary particle hydrodynamic radius (van Zanten and Elimelech 1992). All measurements were carried out at 25°C, and the pH of each of the stock solution and DI water was checked before the experiments. Additionally, the coagulation experiments with organic matter and nanoparticles were conducted under various aquatic conditions. The effect of pH on the coagulation was tested by altering the hydrogen content with HNO_3 and NaOH. To

test the effect of divalent anions, Na_2SO_4 was added to the samples under various concentrations.

3.4 Sedimentation experiments

For large organic matter, a differential sedimentation method was applied to measure the amount of sorption onto sludge flocs. The method was based on a method developed by Nicolosi *et al.* (2005) measuring the sedimentation as a function of time. Examples of the process are illustrated in a previous research conducted by the current research group (Nicolosi *et al.* 2005). To obtain a sediment curve, a time dependent measurement of turbidity should be conducted. Samples were mixed in 12 mm disposable polystyrene cuvettes, where sludge and ENP were added along with DI water and NaCl, depending on the experiment. The cuvettes where shaken and placed on a shaking plate for 2 hr. The cuvettes where then placed in a UV-visible spectrophotometer (HACH DR5000) to measure the light transmittance at the wavelength of 600 nm. The light transmittance was recorded every 10 min for the first 1hr, 20 min for the next 1 hr, and every 30 min for the next 2 hours. Each experiment was repeated 5 times for accuracy. A sedimentation curve was plotted based on the measured transmittance values. The sediment curve was separated into various sections based on the type of sediment. Free ENP concentration was extrapolated based on the final section of the sediment curve, which represents free floating ENP. The attached amount of ENP was calculated by subtracting the free ENP concentration from the added initial ENP concentration.

4. Result and discussion

4.1 Interaction of engineered nanoparticles under various aquatic conditions

The stability of nanoparticles is closely related to the fate, and transport, of nanoparticles. Previous research has shown that aquatic conditions such as ionic strength, organic matter, and divalent cations are the main factors influencing particle stability. However, previous research mainly focuses on a single organic matter under low concentrations, which may not properly represent the field conditions. So in the current study particle stability was tested under conditions simulating filed conditions, such as neutral pH, and high DOM concentrations. Conditions such as the pH and type of ions were considered in the experiment. The results of this study will aid in the comprehension and prediction of ENP in wastewater treatment plants, providing insight to particle interaction under field conditions.

Fig. 1, shows the increase of $nTiO_2$ particle size as a function of time. The experiments were performed in duplicates at each electrolyte concentration showing good reproductively. Results showed an increase in the hydrodynamic radius with time for different electrolyte concentrations. The slope of the hydrodynamic radius versus time curve increased dramatically when the electrolyte concentration was increased from 0.01 M to 0.1 M. Any increase in the electrolyte concentration did not result in an incline in the slope indicating that 0.1 M NaCl is in the fast aggregation regime. This is in good agreement with the characteristics of the fast regime where the coagulation rate constant is independent of the electrolyte concentrations. It can also be observed that at higher electrolyte concentrations the particle size distribution increases with time. This is due to multiple scattering, which leads to a diffuse halo around the primary laser beam inside the cell and a reduced intercept of the autocorrelation function resulting in a wider spread in particle size measurement.

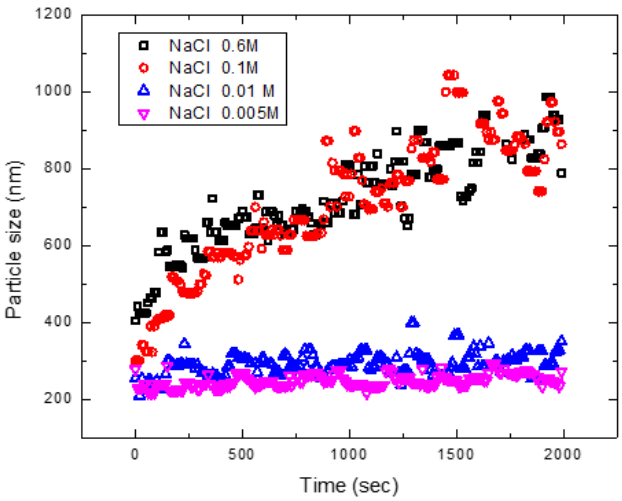

Fig. 1 Dynamic light scattering (DLS) measurements of $nTiO_2$ aggregation. The aggregation profile was measured as a function of salt concentration; Conditions: TiO_2 = 10mg/L, pH = 8, NaCl used as an electrolyte

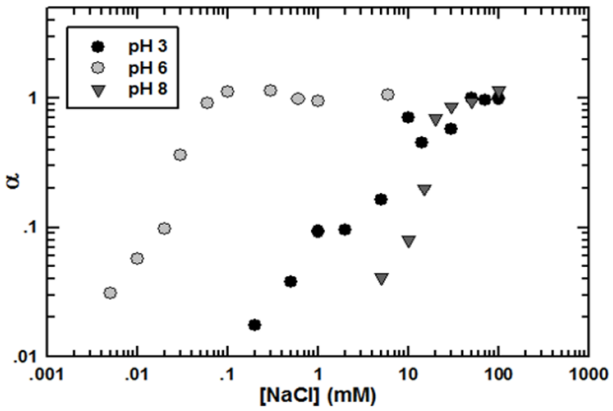

Fig. 2 Stability ratio as a function of various pH conditions; The blue dashed line indicates the CCC value at pH 6, the purple double dotted line indicates the CCC value at pH 3, and the red dotted line indicates the CCC value at pH 8 Experimental conditions: [TiO_2] = 80 mg/L; Temperature = 25°C; electrolyte = NaCl

From the slopes obtain in Fig. 1 the attachment efficiency was calculated and presented in Fig. 2. The stability ratio was shown through the attachment efficiency as a function of electrolyte concentration. Fast coagulation (where the attachment efficiency = 1) was calculated by averaging three of the slopes in the fast regime. The effect

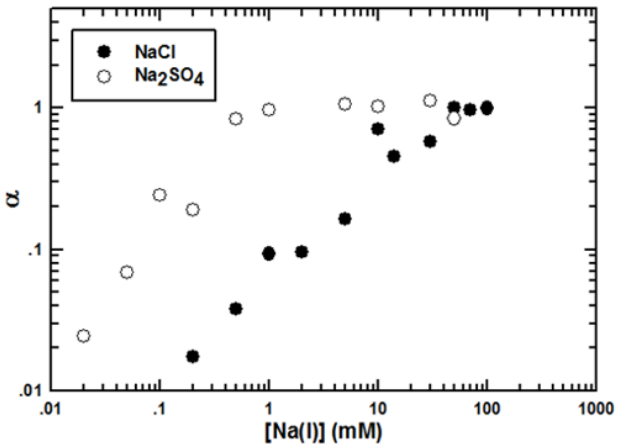

Fig. 3 Stability ratio ratio as a function of electrolyte concentration; The solid line indicates the CCC value with Na_2SO_4 added, where the dashed line indicates the CCC value when NaCl is added; Experimental conditions [TiO_2] = 80 mg/L; Temperature = 25°C; pH = 3

of pH on particle aggregation was verified by testing the attachment efficiency of TiO_2 in three different pH conditions (pH 3, 6, 8). The pH was selected based on the zero point charge (ZPC) of the particles, which is known to be approximately pH 6.3. Zeta potential of the particles were measured at +15mV for pH 3, close to zero at pH 6, and -20mV at pH 8. Coagulation of the particles show a strong correlation with the zeta potential where the attachment efficiency was 0.07 mM at pH 6, 8 mM at pH 3, and 20mM for pH 8. Based on the degree of surface charge, the CCC value rises from one to two degrees of magnitude. The effect of pH can be seen with the results where the surface charge is a two-step protonation of the metal oxides on the particle surface. Since pH 6 is near neutral conditions, a slight increase of ionic strength will result in the coagulation of the particles due to the even distribution of single protonated surface groups. However, with pH 3 the high concentration of dual-protonated surface charges demands a higher degree of anions to suppress the positive surface charge. And with particles in pH 8, the cations will interact with the deprotonated surface for coagulation.

Aside from the effect of pH and salinity, multivalent ions are also known to have pronounced effects on the destabilization of colloidal particles (Gambinossi *et al.* 2015). Fig. 3 shows the aggregation profiles with different divalent anion concentrations at pH 3 where the particles displayed a positive charge. Results showed a rapid increase in the slope at Na_2SO_4 concentrations up to 0.5 mM. Compared with the monovalent anions the divalent anions showed a difference in the CCC up to two degrees of magnitude. Shih *et al.* (2012) have also reported similar results where the CCC of NaCl was 8.2 mM and $NaSO_4^{2-}$ was 0.05 mM. The results with Cl^- showed almost identical results where SO_4^{2-} showed a one degree of magnitude difference. This may be due to the fact that Shih *et al.* (2012) conducted the experiments in pH 3 to 4, where in pH 4 the zeta potential dropped to 8 mV aiding in the lower CCC value. However, in various researches the effect of divalent cations have shown to differ based on the selected ionic species. Results have indicated that will various divalent ionic species the CCC values may differ up to two degrees in magnitude (French *et al.* 2009, Keller *et al.* 2010, Thio *et al.* 2011). The Schulze–Hardy rule states that the difference between the monovalent and divalent ion CCC values should be 1:64 (1/16:1/26). However, the results from the two different electrolytes (Cl^- and SO_4^{2-}) show a ratio of 1:16.4. The difference between the theoretical and experimental value may be due to the size and symmetry of the sulfate ions, where the Schulze–Hardy rule is based on the assumption of using symmetrical ions, not fitting the tetratomic ions of interest (Thio *et al.* 2011).

4.2 Interaction of engineered nanoparticles and dissolved organic matter

The effect of dissolved organic matter on particle stability was tested with organic matter sampled from a wastewater treatment plant. Dissolved organic matter was extracted from secondary waste sludge and tested under the sampled pH conditions (pH 6). The DOM showed TOC concentrations of 409 mg/L, where the experimental conditions were set at 300 mg/L due to the addition of ENP and ionic species.

Fig. 4 shows the attachment efficiency of $nTiO_2$ and nZnO under various DOM concentrations. With dissolved organic matter, results showed that both particles displayed higher CCC values. The overall aggregation kinetics of both particles showed similar results, where CCC values where of NaCl concentrations of 100 mM. However as seen in Fig. 4(a), the change in organic matter concentration impacts the aggregation kinetics, where lower organic concentration shows lower CCC values. It has been proven in previous studies that the amount of sorption influences the aggregation kinetics of nanoaprticles, where increasing HA concentrations from 1 mg/L to 5 mg/L results in a 35% increase in the CCC (Erhayem and Sohn 2014). This may be due to the compact formation of DOM on particle surfaces where the increase of ionic strength impacts the shape and morphology of organic material. It has been reported that with increased ionic strength, the steric repulsion of humic acid (HA) decreases, resulting in a compact sorption layer of HA on the particle surface (Yuan *et al.* 2008, Liao *et al.* 2017). Higher ionic strength may also change the shape of the organic material from linear to spherical due to the neutralization of anionic carboxylic and phenolic groups resulting in higher sorption (Wang *et al.* 2001, Erhayem and Sohn 2014). Hence, higher ionic strength and organic concentration may result in the decrease of aggregation kinetics.

Additionally, the concentration of DOM may also be a factor, where with higher DOM attachments will lead to an increased in the number of functional sites, requiring a higher amount of cations to reduce the steric effects of the organic material.

By comparing Figs. 4 (a) and 4(b) it can be seen that interactions with the DOM, sampled from wastewater treatment plants, resulted in similar CCC values for both TiO_2 and ZnO. It should be mentioned that the surface charge of the two ENPs are different where ZnO shows strong positive charge, and TiO_2 a near neutral charge.

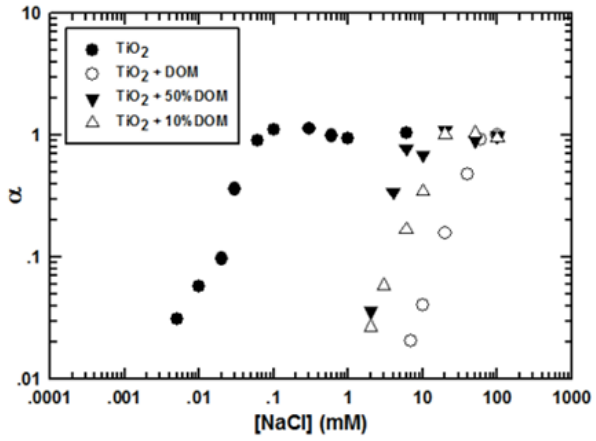

(a) Interaction of TiO_2 and DOM

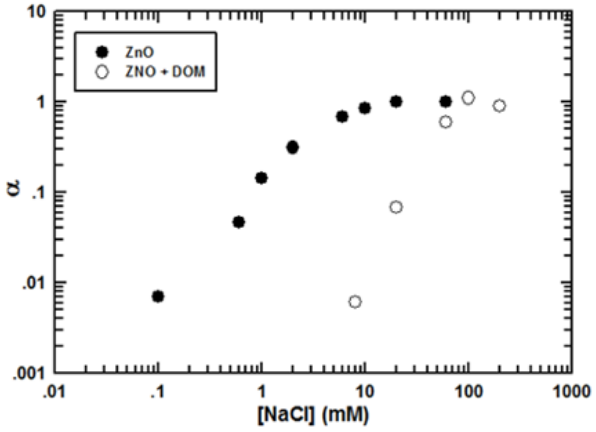

(b) Interaction of ZnO and DOM

Fig. 4 Stability ratio as a function of various DOM conditions; Experimental conditions: [TiO_2] = 50 mg/L; [ZnO] = 50 mg/L; Temperature = 25°C; electrolyte = NaCl; DOM = 300 mg/L; pH 6

Regardless of the nanoparticle surface charge the stability of the particles will rely on the steric repulsion of the organic matter. And due to the fact that both particles displayed stability values near 100mM, it can be deduced that equal amounts of functional groups are displayed on the outer organic layer. Additionally, it can also be deduced that for similar steric repulsion to occur, the amount of organic sorption is higher with positively charged particles to mask the surface charge. This may be due to the masking of the particle surface charge. And at the surface of the particles, similar amounts of functional groups are exposed to the aquafer resulting in similar stability of the particles. Particles of different surface charges may have different DOM sorption capacities, where the positively charged particles have larger amounts of DOM attachment to mask the surface charge (Gora and Andrews 2017). This may lead to the fact that regardless of the particle type, high concentrations of dissolved organic matter will cancel out the particle surface charge effect. So based on the results above it can be concluded that under field conditions, regardless of the surface charge or material composition of the ENP, DOM attachment leads to a similar degree of stability for various nanoparticles.

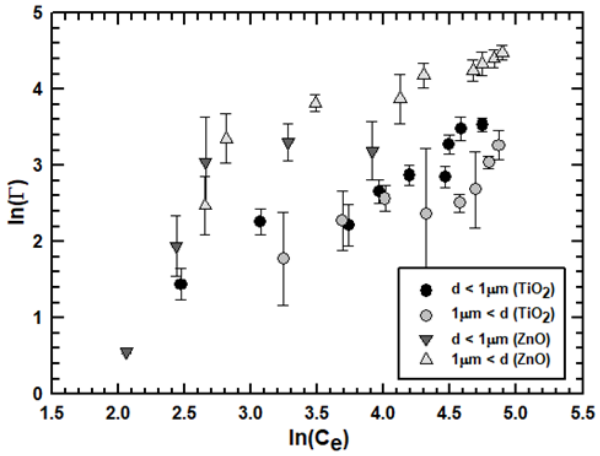

Fig. 5 Sorption study of DOM and small organic particulates with $nTiO_2$ and nZnO; Small organic particulate matter (d < 1μm), Large organic particulate matter (d > 1μm), pH 6.5; (a) Organics obtained from primary waste sludge; (b) Organics obtained from secondary waste sludge

4.3 Interaction of engineered nanoparticles and organic particulates

As it can be seen in Fig. 4, both particles display similar CCC values under the presence of high DOM concentrations although $nTiO_2$ and nZnO have different surface charges. Based on the results, organic sorption experiments were conducted under the assumption that the affinity of ENP to organic matter will depend on the particle surface charge. To verify the assumption, sorption experiments were conducted on both $nTiO_2$ and nZnO with organic matter from wastewater treatment plants.

Fig. 5 compares the attachment of $nTiO_2$ and nZnO onto wastewater sludge and its constituents. Since the interaction of dissolved organic matter and ENP have been observed in the previous section, ENP interaction with particulate organic matter was observed to better understand the interaction and fate of the nanoparticles. Wastewater sludge was separated into two size groups, small organic particular matter (d < 1 μm) and large organic particular matter (d > 1 μm), to undergo sorption experiments with ENP. Results show that for both large and small organic particulates, nZnO display a stronger affinity than $nTiO_2$. This has also been observed in various studies, where the maximum sorption of humic acid (HA) to nZnO was measured to be 60.48 mgHA/gNP (Zhou and Keller 2010), and maximum NOM sorption to $nTiO_2$ of 18 mg NOM/gNP (Erhayem and Sohn 2014). Although it has been proven that humic acids have a stronger affinity to metallic particles, the measured difference does not exceed two times the amount (Erhayem and Sohn 2014). The difference in the affinity is mainly due to the positive surface charge of nZnO, compared to $nTiO_2$ displaying a nearly neutral surface charge. The negative charge of organic matter induces the attachment of nZnO onto the organic surfaces. Attachment of nZnO to organic particulates will result in charge screening, where the compiling of the particles masks the negative charge of the

functional groups favoring additional attachment of nZnO onto the organic material. This may lead to a multilayer sorption, where the positive surface charge masks the functional groups of the organic layer leading to additional nZnO attachment. Additionally, the stronger positive charge contributes to smaller and more mobile nZnO nanoparticles. The lack of aggregation will provide a larger surface area, compared to $nTiO_2$, leading to higher amount of DOM attachment to nZnO surfaces.

It can also be seen in Fig. 5 that large organic particulates have a higher affinity with nZnO. This is due to the existence of DOM in the small organic particular samples, and its attachment to the ZnO surfaces. Attachment of DOM to ZnO surfaces hinders the positive charge of the nanoparticles stabilizing it thorough steric hindrance. This prevents the attachment of ZnO to small organic particular matter, hence the lower sorption results of ZnO to small organic particular matter. However, with nanoparticles and larger organic flocs, various mechanism occurs with the interaction resulting in higher amounts of nZnO attachment to the organic matter. Studies have shown that nanoparticles can be found in wastewater samples through floc aggregation, microbial cell attachment, and internalization within microbial cells (Chowdhury *et al*. 2012, Park *et al*. 2013). For floc aggregation, positively charged particles have been proven to increase the floc size through the reduction of the organic material's energy barrier resulting in a fractal shape aggregation of the flocs (Mukha *et al*. 2013, Xu and Li 2016). Aside from the attachment of nanoparticles to various wastewater constituents, nanoparticles have also been proven to penetrate through the microbe membrane and entrapped inside the cells. Due to the combined effects stated above, nZnO may show higher degrees of attachment to larger organic matter.

Aside from the interactions mentioned above, the complexity of ENP sorption to wastewater organic matter may be due to various reasons other such as calcium bridging, ligand exchange, chelation, and hydrophobic attraction. Further research is to be conducted on the matter.

5. Conclusions

In the current research the stability of ENP was tested under various aquatic conditions simulating field conditions. CCC experiments with pH and ionic strengths showed results that agreed with conventional DVLO theories. However, with the addition of DOM, both tested nanoparticles ($nTiO_2$, nZnO) showed similar CCC values. This indicates that at field conditions, where the DOM concentration is high and the organic composition is diverse, the attachment of DOM to nanoparticles may differ based on the nanoparticle surface charge. The positive surface charge of nZnO attracts higher amounts of DOM to the surface, leading to a multi-layer attachment of organic matter. The attachment of the organic layers proceeds to the point where the functional groups of the organic matter maximizes on the outer sorption layer, where nZnO attracts more organic matter due to its positive surface charge. Different amount in organic attachment and its influence in particle stability can also be seen in Fig. 4(a), where at lower DOM concentrations the CCC values of the nanoparticles decrease. This may also be explained with the amount of functional groups on the outer sorption layer since with lower DOM concentrations the amount of DOM sorption will decrease, hence lesser number of functional groups will be positioned at the outer sorption layer. In conclusion, although ENPs of various materials and surface charges may enter the wastewater treatment plants, the organic matter will stabilize the particles in a similar manner, resulting in a plant wide distribution of the ENP.

With DOM, it has been proven that the concentration of the organic matter is the main factor that influences the fate and transport of the nanoparticles. However, with organic particulates it has been proven that the surface charge of the nanoparticles is the main factor that influences the sorption of ENP to organic particulates. Particles with positive surface charges showed higher affinity to the negative organic particulates, displaying attachments of one degree of magnitude higher than neutral particles ($nTiO_2$). This was observed with organic matter of both large and small sizes, where it is assumed that the positive nZnO may form multiple layers on the organic particulate. Additionally, lower degrees of aggregation of ZnO, due to its positive charge, may also aid the higher degree of attachment due to its higher diffusive characters.

With the current research, various aspects of ENP and organic material interaction have been addressed. It should be mentioned that the current research focused on the interaction of ENP with various organic matter sampled directly from wastewater treatment plants. Results have shown high stability of ENP leading to a plant wide distribution of particles. Additionally, the attachment of ENP to large organic matter which indicated accumulation of nanoparticles in the sedimentation tanks.

Acknowledgments

We thank Dr. Rovshan Madmudov and Mr. Michael Davidson for assistance with the ICP throughout the entire research. This work was supported by a STAR grant R83485901 by the US Environmental Protection Agency. The work was also supported by Chungnma National University grant 2019-0905-01. Last but not the least, we wish to thank our project managers, Dr. Nora Savage and Dr. Mitch Lasat for their interest and support of this research.

References

Aboubaraka, A.E., Aboelfetoh, E.F. and Ebeid, E.Z.M., (2017), "Coagulation effectiveness of graphene oxide for the removal of turbidity from raw surface water", *Chemosphere*, **181**, 738-746. https://doi.org/10.1016/j.chemosphere.2017.04.137.

Adams, L.K., Lyon, D.Y. and Alvarez, P.J.J., (2006), "Comparative eco-toxicity of nanoscale TiO_2, SiO_2, and ZnO water suspensions", *Water Res*., **40**(19), 3527-3532. https://doi.org/10.1016/j.watres.2006.08.004.

Benn, T., Cavanagh, B., Hristovski, K., Posner, J.D. and Westerhoff, P. (2010), "The release of nanosilver from

consumer products used in the home", *J. Environ. Qual.*, **39**(6), 1875. https://doi.org/10.2134/jeq2009.0363.

Benn, T.M. and Westerhoff, P. (2008), "Nanoparticle silver released into water from commercially available sock fabrics", *Environ. Sci. Technol.*, **42**(11), 4133-4139. https://doi.org/10.1021/es7032718.

Bolyard, S.C., Reinhart, D.R. and Santra, S. (2013), "Behavior of engineered nanoparticles in land fill leachate", *Environ. Sci. Technol.*, **47**(15), 8114. https://doi.org/10.1021/es305175e.

Bundschuh, M., Filser, J., Lüderwald, S., McKee, M.S., Metreveli, G., Schaumann, G.E., Schulz, R. and Wagner, S. (2018), "Nanoparticles in the environment: where do we come from, where do we go to?", *Environ. Sci. Eur.*, **30**(1), 1-17. https://doi.org/10.1186/s12302-018-0132-6.

Chang, H.H., Cheng, T.J., Huang, C.P. and Wang, G.S. (2017), "Characterization of titanium dioxide nanoparticle removal in simulated drinking water treatment processes", *Sci. Total Environ.*, **601-602**, 886-894. https://doi.org/10.1016/j.scitotenv.2017.05.228.

Chen, K.L. and Elimelech, M., (2006), "Aggregation and deposition kinetics of fullerene (C-60) nanoparticles", *Langmuir*, **22**(18), 10994-11001. https://doi.org/10.1021/la062072v.

Chen, K.L. and Elimelech, M., (2007), "Influence of humic acid on the aggregation kinetics of fullerene (C60) nanoparticles in monovalent and divalent electrolyte solutions", *J. Colloid Interf. Sci.*, **309**(1), 126-134. https://doi.org/10.1016/j.jcis.2007.01.074.

Chen, K.L., Mylon, S.E. and Elimelech, M. (2007), "Enhanced aggregation of alginate-coated iron oxide (Hematite) nanoparticles in the presence of calcium, strontium, and barium cations enhanced aggregation of alginate-coated iron oxide (Hematite) nanoparticles in the presence of calcium, strontium", *Society*, **17**(6), 5920-5928. https://doi.org/10.1021/la063744k.

Chowdhury, I., Duch, M.C., Mansukhani, N.D., Hersam, M.C. and Bouchard, D. (2013) "Colloidal properties and stability of graphene oxide nanomaterials in the aquatic environment", *Environ. Sci. Technol.*, **47**(12). https://doi.org/10.1021/es400483k.

Chowdhury, I., Cwiertny, D.M. and Walker, S.L. (2012), "Combined factors influencing the aggregation and deposition of nano-TiO_2 in the presence of humic acid and bacteria", *Environ. Sci. Technol.*, **46**(13), 6968-6976. https://doi.org/10.1021/es2034747.

Debia, M., Bakhiyi, B., Ostiguy, C., Verbeek, J.H., Brouwer, D.H. and Murashov, V. (2016), "A systematic review of reported exposure to engineered nanomaterials", *Annals of Occup. Hyg.*, **60**(8), 916-935. https://doi.org/10.1093/annweh/wxy048.

Duch, M.C., Budinger, G.R.S., Liang, Y.T., Soberanes, S., Urich, D., Chiarella, S.E., Campochiaro, L.A., Gonzalez, A., Chandel, N.S., Hersam, M.C. and Mutlu, G.M. (2011), "Minimizing oxidation and stable nanoscale dispersion improves the biocompatibility of graphene in the lung", *Nano Lett.*, **11**(12), 5201-5207. https://doi.org/10.1021/nl202515a.

Erhayem, M. and Sohn, M. (2014), "Stability studies for titanium dioxide nanoparticles upon adsorption of Suwannee River humic and fulvic acids and natural organic matter", *Sci. Total Environ.*, **468-469**, 249-257. https://doi.org/10.1016/j.scitotenv.2013.08.038.

French, R.A., Jacobson, A.R., Kim, B., Isley, S.L., Penn, R.L. and Baveye, P.C. (2009), "Influence of ionic strength, pH, andcation valence on aggregation kinetics of titanium dioxide nanoparticles", *Environ. Sci. Technol.*, **43**(5), 1354-1359. https://doi.org/10.1021/es802628n.

Gambinossi, F., Mylon, S.E. and Ferri, J.K. (2015) "Aggregation kinetics and colloidal stability of functionalized nanoparticles", *Adv. Colloid Interf. Sci.*, **222**, 332-349. https://doi.org/10.1016/j.cis.2014.07.015.

Gora, S.L. and Andrews, S.A. (2017), "Adsorption of natural organic matter and disinfection byproduct precursors from surface water on TiO_2 Nanoparticles: pH effects, isotherm modelling and implications for using TiO_2 for drinking water treatment", *Chemosphere.*, **174**, 363-370. https://doi.org/10.1016/j.chemosphere.2017.01.125.

Hansen, F.S. Heggelund, L.R., Besora, P.R., Mackevica, A., Boldrina, A. and Bauna, A. (2016), "Nanoproducts - What is actually available to European consumers?", *Environ. Sci. Nano.*, **3**(1), 169-180. https://doi.org/10.1039/C5EN00182J.

Illés, E. and Tombácz, E. (2006), "The effect of humic acid adsorption on pH-dependent surface charging and aggregation of magnetite nanoparticles", *J. Colloid Interf. Sci.*, **295**(1), 115-123. https://doi.org/10.1016/j.jcis.2005.08.003.

Jiang, Y., Raliya, R., Fortner, J.D., Biswas, P. (2016), "Graphene oxides in water: Correlating morphology and surface chemistry with aggregation behavior." *Environ. Sci. Technol.*, **50**(13), 6964-6973. https://doi.org/10.1021/acs.est.6b00810.

Kaegi, R., Ulrich, A., Sinnet, B., Vonbank, R., Wichser, A., Zuleeg, S., Simmler, H., Brunner, S., Vonmont, H., Burkhardt, M. and Boller, M. (2008), "Synthetic TiO_2 nanoparticle emission from exterior facades into the aquatic environment", *Environ. Pollut.*, **156**(2), 233-239. https://doi.org/10.1016/j.envpol.2008.08.004.

Keller, A.A., Wang, H., Zhou, D., Lenihan, H. S., Cherr, G., Cardinale, B.J., Miller, R., and Ji, Z. (2010), "Stability and aggregation of metal oxide nanoparticles in natural aqueous matrices", *Environ. Sci. Technol.*, **44**(6), 1962-1967. https://doi.org/10.1021/es902987d.

Li, K. and Chen, Y. (2012), "Effect of natural organic matter on the aggregation kinetics of CeO_2 nanoparticles in KCl and $CaCl_2$ solutions: Measurements and modeling", *J. Hazard. Mater.*, **209-210**, 264-270. https://doi.org/10.1016/j.jhazmat.2012.01.013.

Li, M. and Huang, C.P. (2010), "Stability of oxidized single-walled carbon nanotubes in the presence of simple electrolytes and humic acid", *Carbon.*, **48**(15), 4527-4534. https://doi.org/10.1016/j.carbon.2010.08.032.

Liao, P., Li, W., Wang, D., Jiang, Y., Pan, C., Fortner, J.D. and Yuan, S. (2017), "Effect of reduced humic acid on the transport of ferrihydrite nanoparticles under anoxic conditions", *Water Res.*, **109**, 347-357. https://doi.org/10.1016/j.watres.2016.11.069.

Miao, L., Wang, C. and Xu, Y. (2016), "Effect of alginate on the aggregation kinetics of copper oxide nanoparticles (CuO NPs): bridging interaction and hetero-aggregation induced by Ca^{2+}", *Environ. Sci. Pollut. Res.*, **23**(12), 11611-11619. https://doi.org/10.1007/s11356-016-6358-1.

Mukha, I.P., Eremenko, A.M., Smirnova, N.P., Mikhienkova, A.I., Korchak, G.I., Gorchev, V.F. and Chunikhin, A.I. (2013), "Antimicrobial activity of stable silver nanoparticles of a certain size", *Appl. Biochem. Microbiol.*, **49**(2), 199-206. https://doi.org/10.1134/S0003683813020117.

Nicolosi, V., Vrbanic, D., Mrzel, A., McCauley, J., O'Flaherty, S., McGuinness, C., Compagnini, G., Mihailovic, D., Blau, W.J. and Coleman, J.N. (2005), "Solubility of Mo6S4.5I4.5 nanowires in common solvents: A sedimentation study", *J. Phys. Chem. B*, **109**(15), 7124-7133. https://doi.org/10.1021/jp045166r.

Nowack, B., Krug, H. and Height, M. (2011), "120 Years of nanosilver history: Implications for policy makers", *Environ. Sci. Technol.*, **45**(7), 3189. https://doi.org/10.1021/es200435m.

Park, H.J., Kim H.Y., Cha, S., Ahn, C.H., Roh, J., Park, S., Kim, S., Choi, K., Yi, J., Kim, Y. and Yoon, J. (2013), "Removal characteristics of engineered nanoparticles by activated sludge", *Chemosphere*, **92**(5), 524-528. https://doi.org/10.1016/j.chemosphere.2013.03.020.

Petersen, E.J., Zhang, L., Mattison, N.T., O'Carroll, D.M., Whelton, A.J., Uddin, N., Nguyen, T., Huang, Q., Henry, T.B., Holbrook, R.D. and Chen, K.L. (2011), "Potential release pathways, environmental fate, and ecological risks of carbon nanotubes", *Environ. Sci. Technol.*, **45**(23), 9837. https://doi.org/10.1021/es201579y.

Sani-Kast, N. Labille, J., Ollivier, P., Slomberg, D., Hungerbühler, K. and Scheringer, M. (2017), "A network perspective reveals decreasing material diversity in studies on nanoparticle interactions with dissolved organic matter", *Proceedings of the National Academy of Sciences*, **114**(10), E1756-E1765. https://doi.org/10.1073/pnas.1608106114.

Shih, Y.H., Liu, W.S. and Su, Y.F. (2012), "Aggregation of stabilized TiO_2 nanoparticle suspensions in the presence of inorganic ions", *Environ. Toxicol. Chem.*, **31**(8), 1693-1698. https://doi.org/10.1002/etc.1898.

Sousa, V.S., Corniciuc, C. and Ribau Teixeira, M. (2017), "The effect of TiO2nanoparticles removal on drinking water quality produced by conventional treatment C/F/S", *Water Res.*, **109**, 1-12. https://doi.org/10.1016/j.watres.2016.11.030.

Sun, T.Y., Bornhöft, N.A., Hungerbühler, K. and Nowack, B. (2016), "Dynamic probabilistic modeling of environmental emissions of engineered nanomaterials", *Environ. Sci. Technol.*, **50**(9), 4701-4711. https://doi.org/10.1021/acs.est.5b05828.

Thio, J.R., Zhou, D. and Keller, A.A. (2011), "Influence of natural organic matter on the aggregation and deposition of titanium dioxide nanoparticles", *J. Hazard. Mater.*, **189**(1-2), 556-563. https://doi.org/10.1016/j.jhazmat.2011.02.072.

Müller, T.J.J., Bunz, U.H.F. (2007), *Functional Organic Materials: Syntheses, Strategies and Applications*, John Wiley & Sons, Morlenbach, Germany.

Wagener, S., Dommershausen, N., Jungnickel, H., Laux, P., Mitrano, D., Nowack, B., Schneider, G. and Luch, A. (2016), "Textile functionalization and its effects on the release of silver nanoparticles into artificial sweat", *Environ. Sci. Technol.*, **50**(11), 5927-5934. https://doi.org/10.1021/acs.est.5b06137.

Wang, Y., Combe, C. and Clark, M.M. (2001), "The effects of pH and calcium on the diffusion coefficient of humic acid", *J. Membr. Sci.*, **183**(1), 49-60. https://doi.org/10.1016/S0376-7388(00)00555-X.

Weir, A. Westerhoff, P., Fabricius, L., Hristovski, K. and Goetz, N.V. (2012), "Titanium dioxide nanoparticles in food and personal care products", *Environ. Sci. Technol.*, **46**(4), 2242-2250. https://doi.org/10.1021/es204168d.

Windler, L., Lorenz, C., Goetz, N.V., Hungerbühler, K., Amberg, M., Heuberger, M. and Nowack, B. (2012), "Release of titanium dioxide from textiles during washing", *Environ. Sci. Technol.*, **46**(15), 8181-8188. https://doi.org/10.1021/es301633b.

Xu, J. and Li, X.Y. (2016), "Investigation of the effect of nanoparticle exposure on the flocculability of activated sludge using particle image velocimetry in combination with the extended DLVO analysis", *Colloid Surfaces B*, **143**, 382-389. https://doi.org/10.1016/j.colsurfb.2016.03.062.

Yuan, B., Pham, M. and Nguyen, T.H. (2008), "Deposition kinetics of bacteriophage MS2 on a silica surface coated with natural organic matter in a radial stagnation point flow cell", *Environ. Sci. Technol.*, **42**(20), 7628-7633. https://doi.org/10.1021/es801003s.

Van Zanten, J.H. and Elimelech, M. (1992), "Determination of absolute coagulation rate constants by multiangle light scattering", *J. Colloid Interf. Sci.*, **154**(1), 1-7. https://doi.org/10.1016/0021-9797(92)90072-T.

Zheng, X., Wu, R. and Chen, Y. (2011), "Effects of ZnO nanoparticles on wastewater biological nitrogen and phosphorus removal", *Environ. Sci. Technol.*, **45**(7), 2826-2832. https://doi.org/10.1021/es2000744.

Zhou, D. and Keller, A.A. (2010), "Role of morphology in the aggregation kinetics of ZnO nanoparticles", *Water Res.*, **44**(9), 2948-2956. https://doi.org/10.1016/j.watres.2010.02.025.

YP